

PAPER • OPEN ACCESS

## A graphene-modified Co-BDC metal-organic frameworks (Co-MOF) for electrochemical non-enzymatic glucose sensing

To cite this article: R Yuniasari *et al* 2021 *IOP Conf. Ser.: Mater. Sci. Eng.* **1045** 012010

View the [article online](#) for updates and enhancements.



**ECS** **240th ECS Meeting**  
Oct 10-14, 2021, Orlando, Florida

**Register early and save  
up to 20% on registration costs**

Early registration deadline Sep 13

**REGISTER NOW**

# A graphene-modified Co-BDC metal-organic frameworks (Co-MOF) for electrochemical non-enzymatic glucose sensing

R Yuniasari<sup>1</sup>, F Amri<sup>1</sup>, S A Abrori<sup>1</sup>, N L W Septiani<sup>1</sup>, M Rezki<sup>1</sup>, Irzaman<sup>2</sup>, M Z Fahmi<sup>3</sup> and B Yulianto<sup>\*,1,4</sup>

<sup>1</sup> Department of Engineering Physics, Faculty of Industrial Technology, Institute of Technology Bandung, Bandung 40132, Indonesia.

<sup>2</sup> Department of Physics, Faculty of Mathematics and Natural Sciences, Bogor Agricultural University, Bogor, Indonesia.

<sup>3</sup> Department of Chemistry, Faculty of Science and Technology, Universitas Airlangga, Surabaya 60115, Indonesia.

<sup>4</sup> Research Center for Nanoscience and Nanotechnology (RCNN), Institute of Technology Bandung, Bandung 40132, Indonesia.

\* Corresponding Author: [brian@tf.itb.ac.id](mailto:brian@tf.itb.ac.id)

**Abstract.** In this work, a metal-organic framework (MOF) based on cobalt was decorated with graphene and used as a sensing material for glucose determination with electrochemical principles. The selection of Co-MOF material is based on its porous nature, large surface area, and excellent electrochemical properties. The combination of Co-MOF with graphene (high conductivity) effectively increased the electrochemical sensor current. The fabricated composite owned the good crystallinity with graphene particles attached to the Co-MOF surface. The biosensing performance was evaluated by cyclic voltammetry (CV) with 0.1 M NaOH solution as the bolstering electrolyte. The electrochemical measurement indicated that the prepared materials possessed a well-moved transfer electron between the electrode surface and electrolyte solution. The Co-BDC-3Gr sample obtained the best electrochemical performance with the lowest limit of detection (LOD) of 5.39  $\mu\text{M}$  and the highest sensitivity of 100.49  $\mu\text{A mM}^{-1} \text{cm}^{-2}$ . The selectivity test of the modified Co-MOF was done by comparing the response with other compounds such as dopamine, uric acid, and NaCl. The acquired biosensor had excellent stability, with 93% of the initial response after 30 days of storage.

**Keywords.** Cobalt-metal organic framework, graphene, electrochemical, glucose sensing.

## 1. Introduction

Non-enzymatic glucose sensors have been recently developed to replace an enzymatic glucose sensor. Enzymatic-based sensors are considered less effective and efficient due to many factors that affect the quality of the enzyme and their sensing performance such as temperature, humidity, and pH conditions. Those factors cause several problems including short lifetime, instability, complicated immobilization procedure, high cost, and low reproducibility [1-4]. That technique generally requires glucose oxidase, acting as oxidation of glucose to gluconolactone. In contrast, non-enzymatic glucose sensor becomes popular due to its ability to convert glucose to gluconolactone directly [3-5]. Moreover, this technique also offers high stability, excellent repeatability, and relatively low cost [6].

According to several studies that have been reported, materials containing transition metal catalysts such as cobalt, nickel, iron, noble metals such as palladium, platinum, gold, and carbon nanomaterial



show relatively good performance as a non-enzymatic glucose biosensor [7,8]. Among the types of material, three-dimensional MOF containing metal catalyst provides the large surface area, tunable pore, and plentiful active sites for catalytic activity [9-11]. Cobalt-based MOF (Co-MOF) possesses high catalytic activity in the identification of the chemical and biological compounds. For instance, Li *et al.* developed Co-MOF nanosheet array to identify glucose with great sensitivity of  $10,886 \mu\text{A mM}^{-1} \text{cm}^{-2}$  and low LOD of  $1.3 \text{ nM}$  [12]. Co-MOF developed by Yang *et al.* was reported to show high performance as an  $\text{H}_2\text{O}_2$  sensor with high sensitivity and low LOD of  $83.10 \mu\text{A mM}^{-1} \text{cm}^{-2}$  and  $3.76 \mu\text{M}$ , respectively [9]. Moreover, L-cysteine can also be appropriately detected by Co-MOF with a sensitivity and LOD of  $0.0032 \mu\text{A} \mu\text{M}^{-1}$  and  $1.85 \mu\text{M}$ , respectively [13].

In this study, Co-MOF was synthesized using a solvothermal technique in the presence of graphene as a modifier to be applied as a glucose sensor. Graphene is one of the carbon materials in the form of sheets and has a honeycomb structure of graphite [14]. Graphene owns the high potential to be applied as a sensor material because it has a large surface area, good electrical conductivity, high thermal, and chemical stability [14-17]. Moreover, the high conductivity of graphene supplies more electron channels promoting high electron transfer [18,19]. Alizadeh and co-worker synthesized metal oxide combined with graphene as a non-enzymatic glucose biosensor [20]. CuO/graphene showed a high sensitivity and low LOD of  $2939.24 \mu\text{A mM}^{-1} \text{cm}^{-2}$  and  $0.09 \mu\text{M}$ , respectively. Improvement of charge transfer capability provided by a combination of CuO and graphene sheet was believed as a reason for its high performance of glucose sensor. Another study was carried out by Mehek *et al.*, who combined Co-MOF with graphene to be applied as a methanol sensor [21]. The work reported that graphene could increase the surface area (contact area) and electrochemical response. In this study, graphene-modified Co-MOF was applied as electrochemically non-enzymatic glucose biosensor with excellent sensitivity, selectivity, and stability.

## 2. Experimental Section

### 2.1 Materials

Cobalt (II) nitrate hexahydrate ( $\text{Co}(\text{NO}_3)_2 \cdot 6\text{H}_2\text{O}$ , 99.5%), D(+)-glucose, *N,N*-dimethylformamide (DMF) were purchased from Fujifilm Wako. Benzene-1,4-dicarboxylic acid or terephthalic acid ( $\text{H}_2\text{BDC}$ , 98%), uric acid ( $\text{C}_5\text{H}_4\text{N}_4\text{O}_3$ ,  $\geq 99\%$ ), and dopamine were purchased from Sigma-Aldrich. All chemicals were employed as gained without any purification.

### 2.2 Synthesis of Co-BDC MOF

Co-MOF was synthesized by employing a solvothermal method at  $120^\circ\text{C}$  for 24 hours. Typically, 0.28 grams of  $\text{Co}(\text{NO}_3)_2 \cdot 6\text{H}_2\text{O}$  was added in a solvent which contains 20 ml of DMF and 20 ml of ethanol. Subsequently, 0.5 gram of 1,4-benzene dicarboxylic acid was mixed to the solution and then stirred for 1 h. After dissolving, the mixture solution was poured into 100 mL Teflon autoclave and heated at the destined temperature. The precipitated product obtained after cooling down was laundered employing DMF and ethanol three times, respectively, then was dried overnight.

### 2.3 Synthesis of graphene-modified Co-BDC

The graphene-modified Co-BDC was prepared with a similar procedure as Co-BDC preparation. The dissolving process of  $\text{Co}(\text{NO}_3)_2 \cdot 6\text{H}_2\text{O}$  and 1,4-benzene dicarboxylic acid was followed by the addition of graphene to the mixture with various concentrations of 1, 3, and 5%wt, which then in this report are noted as Co-BDC-1Gr, Co-BDC-3Gr, and Co-BDC-5Gr, respectively. After stirring for an hour, the mixture solution was transferred into 100 mL Teflon autoclave and heated at  $120^\circ\text{C}$  for 24 h. The precipitated product obtained after cooling down was washed using DMF and ethanol three times, respectively, subsequently was dried overnight.

### 2.4 Characterization

The phase and crystal structure of all products were characterized using X-ray diffraction Bruker D8 Advance. The morphological of the products was observed using a scanning electron microscope (SEM)

Hitachi SU3500. The infrared spectra were collected by Fourier transform infrared (FTIR) Shimadzu - Prestige 21. Nitrogen ( $N_2$ ) adsorption-desorption characteristic was performed using Quantachrome Instruments (USA) via the Brunauer-Emmett-Teller (BET) approach.

### 2.5 Electrochemical measurements

There are three electrodes employed to measure the electrochemical properties of all samples. The measurements, including CV and amperometry, were performed using Corrtest 350 with glassy carbon electrode (GCE), platinum wire, and Ag/AgCl acted as the working, counter, and reference electrodes, respectively. Before the measurement, 5 mg of each sample was added in 0.5 mL of distilled water and sonicated to reach a homogenous state. 5  $\mu$ L of the solution was then dropped onto GCE and dried naturally. After completely dried, 2  $\mu$ L of Nafion was added on the surface of the layer and was dried naturally. In this research, 0.1 M of NaOH was employed as an electrolyte, and the glucose solutions with varying concentrations (1-10 mM) were prepared in 0.1 M NaOH.

## 3. Results and Discussion

### 3.1 Synthesis and characterization of hierarchical Co-BDC MOF

The diffraction pattern of graphene-assisted Co-BDC can be observed in figure 1. The MOF crystal formed from the bonding between cobalt metals and BDC ligands are marked by fingerprints peak at  $2\theta$  of  $8.8^\circ$ ,  $11.5^\circ$ ,  $12.0^\circ$ , and  $15.9^\circ$  originating from the diffraction planes of (100), (110), (101), and (200), respectively. The diffraction pattern shown by the Co-BDC-graphene composite is very similar to the pattern of pure Co-BDC. The presence of graphene does not interfere with the crystallinity of Co-BDC. Also, graphene owing a diffraction peak at  $2\theta$  of  $26.3^\circ$  does not indicate its presence in the prepared composite system. It also can be reported that 1 wt%, 3 wt%, and 5 wt% graphene added to the Co-BDC system are small enough to be detected by XRD.

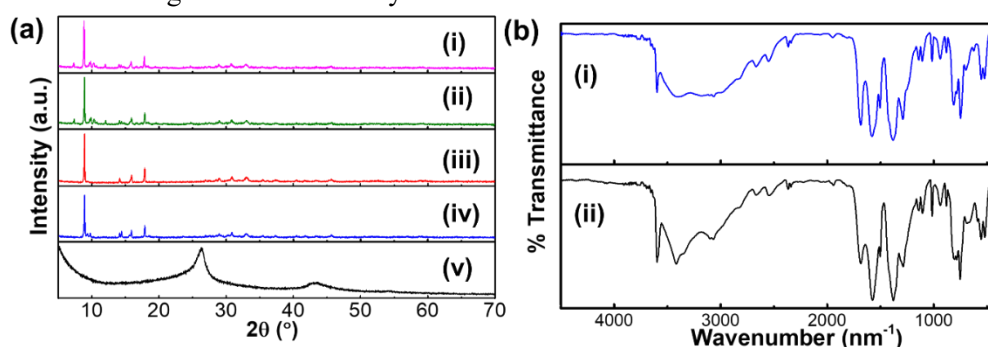


**Figure 1.** (a) Diffraction pattern of Co-BDC MOF (i) and its modification with 1 wt% (ii), 3 wt% (iii), 5 wt% (iv) of graphene in comparison with pure graphene (v). (b) infrared spectrum of Co-BDC (i) in comparison with Co-BDC-3Gr (ii).

Co-BDC or also known as MOF-71, is formed from  $CoO_6$  octahedra chains, and each chain is connected to four other parallel chains by a linker BDC, while the two other sites connect chains in series through DMF [11,22]. Coordination between cobalt and BDC is confirmed through the FTIR spectrum displayed in figure 1b. The infrared spectrum produced by Co-BDC and Co-BDC-graphene composites is relatively similar and showing that the presence of graphene does not interfere with the Co-BDC framework. The sharp peak at  $3700\text{ cm}^{-1}$  originates from OH bound to BDC ligands [23,24]. The broad peak centered at the wavenumber  $3300\text{ cm}^{-1}$  originates from the stretching vibration OH group of water vapor adsorbed on the surface. In contrast, the sharp peak at  $1690\text{ cm}^{-1}$  is derived from stretching vibration group of  $C=O$ . The bond between Co metal and BDC ligands is characterized by the presence of asymmetric and symmetric vibrations  $-COO-$ , respectively in the wavenumber range of  $1575\text{--}1501\text{ cm}^{-1}$  and  $1380\text{ cm}^{-1}$  [25,26]. Hu *et al.* found a decrease in the intensity of the  $C=O$  peak when compared with the same peak in the IR  $H_2BDC$  spectrum showing the interaction between  $Co^{2+}$  and deprotonated  $H_2BDC$  [11]. Co-bonding and BDC ligand are also confirmed by the appearance of peak at  $437\text{ cm}^{-1}$

originating from stretching vibration Co-O. The 3D framework of Co-BDC observed via SEM can be seen in figure 2. Pure Co-BDC has a spindle-like shape with length and diameter of 5  $\mu\text{m}$  and 2.5  $\mu\text{m}$ , respectively.

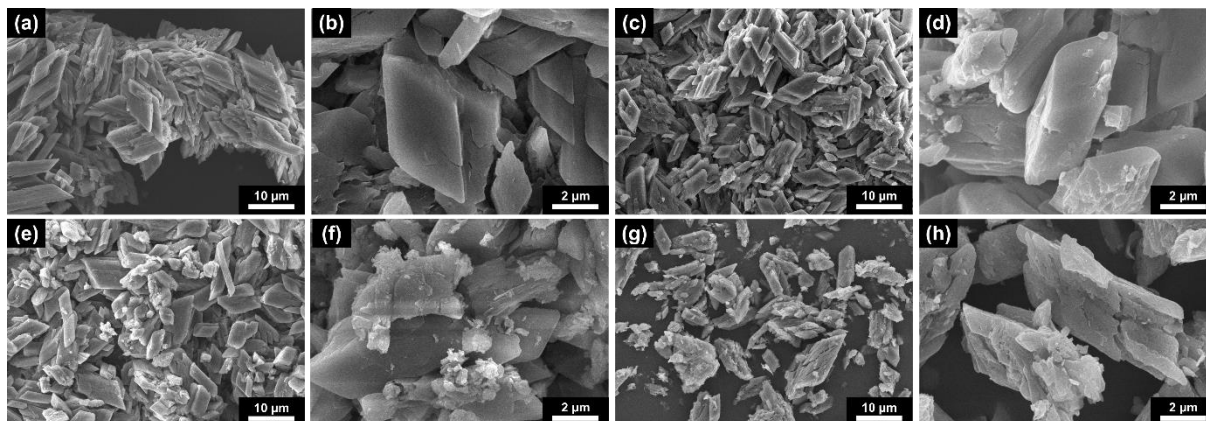


**Figure 2.** SEM images and XRD patterns of obtained Co-MOF and Co-MOF/Gr with the optimized ratios of graphene to Co-BDC: (a,b) Co-BDC, (c,d) Co-BDC-1Gr, (e,f) Co-BDC-3Gr, and (g,h) Co-BDC-5Gr.

Based on the analysis results, the surface of pure Co-BDC looks smooth. This behavior is different from the Co-BDC sample, which has been added by graphene. The surface of the modified Co-BDC looks rougher because there are several particles attached to the surface of the Co-BDC spindle, which is believed to be crumpled of graphene. This structure is reinforced by the increasing number of particles on the Co-BDC surface, along with the increasing amount of graphene given.

$\text{N}_2$  adsorption-desorption technique were employed to calculate the surface area of the as-prepared Co-BDC/Gr samples. From figure 3, the obtained surface area is  $36.2 \text{ m}^2 \text{ g}^{-1}$  and  $36.7 \text{ m}^2 \text{ g}^{-1}$  for Co-BDC and Co-BDC-3Gr, respectively. These results indicate that the addition of graphene does not give a significant effect on the surface area of Co-BDC MOF, even though the graphene has high surface area. This phenomenon strengthens the results of the FTIR analysis earlier.

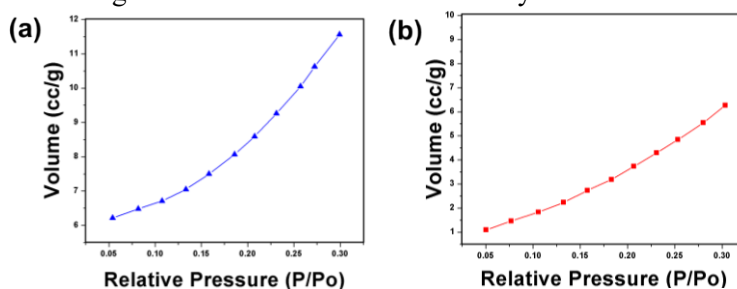


**Figure 3.** Nitrogen adsorption measurement of (a) Co-MOF and (b) Co-MOF-3Gr

### 3.2 Non-enzymatic glucose biosensor performance of hierarchical Co-BDC MOF

The electrochemical property of all samples was evaluated using CV, as shown in figure 4. Oxidation and reduction process of the electrode surface was observed in the potential range of 0-0.8 V in 5 mM glucose solution. There are no oxidation and reduction peaks taking place in the surface of bare GCE and graphene, while oxidation and reduction peaks around 0.4 V and 0.3 V, respectively were observed during the CV process of Co-BDC and Co-BDC-Gr. These peaks also show the increasing of electron transfer, so it can be concluded that the modified electrodes have better electrochemical catalytic properties. The increase of currents in the case of Co-BDC and Co-BDC-Gr are attributed to the change of Co oxidation state from  $\text{Co}^{2+}$  to  $\text{Co}^{3+}$  or vice versa in alkaline media [27]. Addition of graphene to Co-MOF shows an increase in electrochemical sensor activity. Co-MOF can effectively be the active site of the electrode, while graphene increases the electrical conductivity of the sensor. Graphene acts



as a supporting material that increases the electronic conductivity in Co-MOF. Combining the roles and benefits of the two materials causes the Co-MOF/Gr material to have better electrocatalytic properties compared to each material. Furthermore, it is found that the current response peak produced by redox reaction increases along with the increase in the amount of graphene. This situation continues until it reaches the maximum current response in the addition of 3 wt% graphene. At the addition of 5wt% graphene, the resulting current response decreased (figure 4a). Therefore, the addition of 3wt% graphene is the best amount in the electrode system to generate the best performance of the glucose sensor. The effect of scan rates on the CV curve behavior was analyzed mainly for the Co-BDC-3Gr sample (figure 4b). The anodic and cathodic current peaks shift to the right and left side, respectively with increasing of scan rate indicating diffusion-controlled process involved in this glucose detection [28,29].

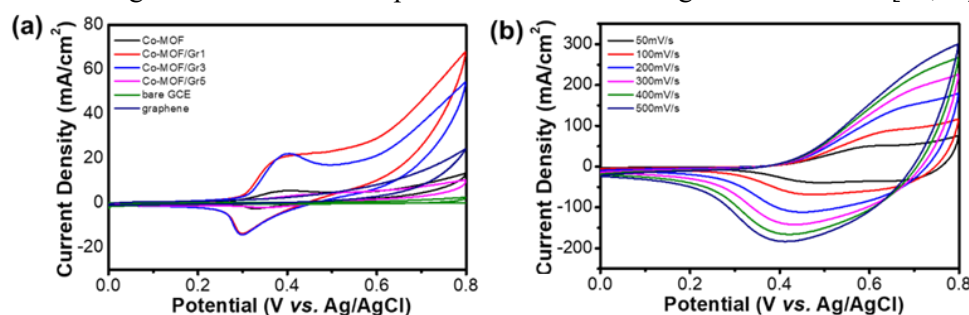


**Figure 4.** Cyclic voltammogram of (a) Co-MOF and Co-MOF/Gr in 5 mM glucose solution with a scan rate of 50 mV.s<sup>-1</sup>. (b) Co-BDC-3Gr with various scan rates.

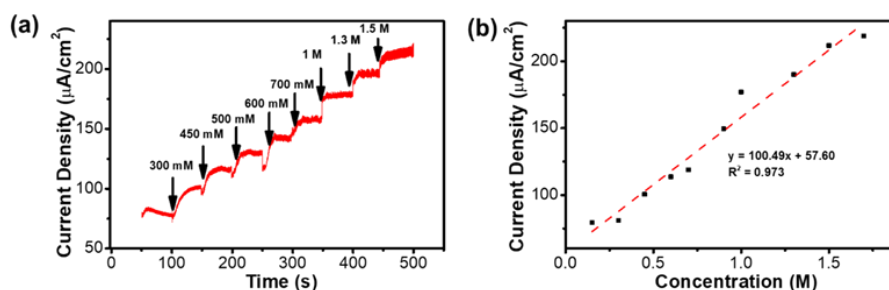


**Figure 5.** (a) Amperometric response and (b) the change in current density of Co-MOF-3Gr.

The amperometric technique can be used to observe the ability of a sensor to produce a direct response to the concentration of analytes. In this case, linearity in sensitivity was determined by making a series of analyte solutions in different concentrations. Figures 5a and 5b show that the current response enhances with increasing concentration of the given glucose solution in the electrolyte solution. This phenomenon causes more ion diffusion to the electrode so that the detected current also increases. The hierarchical Co-BDC MOF sensor shows a sensitivity of 100.49  $\mu\text{A mM}^{-1} \text{cm}^{-2}$  with a correlation coefficient of 0.973. LOD obtained for biosensor is 5.39  $\mu\text{M}$  ( $S/N = 3$ ). The results of biosensor selectivity exhibit excellent performance as indicated by a significant change in current response when injected with glucose compared to other solutions such as dopamine, uric acid, and NaCl. The stability of the Co-BDC-3Gr was evaluated by observing its current response toward 5 mM glucose for several cycles after long-time storage (30 days). The obtained stability of biosensor shows excellent stability, with 93% of the initial response.

#### 4. Conclusion

The Co-MOF-based biosensor platform, combined with graphene for glucose detection, was successfully prepared. The fabricated biosensor has an excellent performance in terms of sensitivity, LOD, selectivity, and stability. Based on the analysis of electrochemical results, the Co-BDC-3Gr sample has the lowest LOD of 5.39  $\mu\text{M}$  with a sensitivity of 100.49  $\mu\text{A mM}^{-1} \text{cm}^{-2}$ . The biosensor

selectivity was tested by comparing the current response between glucose with uric acid, dopamine, and NaCl. The analysis result shows that the biosensor possesses a good selectivity, which is indicated by the most significant current response when injected with a glucose solution. Also, the acquired stability of biosensor exhibits excellent stability, with 93% of the initial response.

### Acknowledgements

This work is partially bolstered by Ministry of Education and Culture, and Ministry of Research and Technology under grant scheme of World Class University (WCU) Program managed by Institute of Technology Bandung (ITB). The authors also acknowledge financial grants provided by ITB, Ministry of Education and Culture, and Ministry of Research and Technology of Indonesia.

### References

- [1] Khosroshahi, Z.; Karimzadeh, F.; Kharaziha, M.; Allafchian, A., A non-enzymatic sensor based on three-dimensional graphene foam decorated with Cu-xCu<sub>2</sub>O nanoparticles for electrochemical detection of glucose and its application in human serum. *Materials Science and Engineering: C* **2020**, *108*, 110216.
- [2] Lin, X.; Wang, Y.; Zou, M.; Lan, T.; Ni, Y., Electrochemical non-enzymatic glucose sensors based on nanocomposite of Co<sub>3</sub>O<sub>4</sub> and multiwalled carbon nanotube. *Chinese Chemical Letters* **2019**, *30* (6), 1157-1160.
- [3] Hwang, D.-W.; Lee, S.; Seo, M.; Chung, T. D., Recent advances in electrochemical non-enzymatic glucose sensors – A review. *Analytica Chimica Acta* **2018**, *1033*, 1-34.
- [4] Zhang, L.; Liang, H.; Ma, X.; Ye, C.; Zhao, G., A vertically aligned CuO nanosheet film prepared by electrochemical conversion on Cu-based metal-organic framework for non-enzymatic glucose sensors. *Microchemical Journal* **2019**, *146*, 479-485.
- [5] Guo, S.; Zhang, C.; Yang, M.; Zhou, Y.; Bi, C.; Lv, Q.; Ma, N., A facile and sensitive electrochemical sensor for non-enzymatic glucose detection based on three-dimensional flexible polyurethane sponge decorated with nickel hydroxide. *Analytica Chimica Acta* **2020**, *1109*, 130-139.
- [6] Ahmad, R.; Tripathy, N.; Ahn, M.-S.; Bhat, K. S.; Mahmoudi, T.; Wang, Y.; Yoo, J.-Y.; Kwon, D.-W.; Yang, H.-Y.; Hahn, Y.-B., Highly Efficient Non-Enzymatic Glucose Sensor Based on CuO Modified Vertically-Grown ZnO Nanorods on Electrode. *Scientific Reports* **2017**, *7* (1), 5715.
- [7] Zhuang, Z.; Su, X.; Yuan, H.; Sun, Q.; Xiao, D.; Choi, M. M. F., An improved sensitivity non-enzymatic glucose sensor based on a CuO nanowire modified Cu electrode. *Analyst* **2008**, *133* (1), 126-132.
- [8] Baghayeri, M.; Amiri, A.; Farhadi, S., Development of non-enzymatic glucose sensor based on efficient loading Ag nanoparticles on functionalized carbon nanotubes. *Sensors and Actuators B: Chemical* **2016**, *225*, 354-362.
- [9] Yang, L.; Xu, C.; Ye, W.; Liu, W., An electrochemical sensor for H<sub>2</sub>O<sub>2</sub> based on a new Co-metal-organic framework modified electrode. *Sensors and Actuators B: Chemical* **2015**, *215*, 489-496.
- [10] Furukawa, H.; Cordova, K. E.; O’Keeffe, M.; Yaghi, O. M., The Chemistry and Applications of Metal-Organic Frameworks. *Science* **2013**, *341* (6149), 1230444.
- [11] Hu, X.; Hu, H.; Li, C.; Li, T.; Lou, X.; Chen, Q.; Hu, B., Cobalt-based metal organic framework with superior lithium anodic performance. *Journal of Solid State Chemistry* **2016**, *242*, 71-76.
- [12] Li, Y.; Xie, M.; Zhang, X.; Liu, Q.; Lin, D.; Xu, C.; Xie, F.; Sun, X., Co-MOF nanosheet array: A high-performance electrochemical sensor for non-enzymatic glucose detection. *Sensors and Actuators B: Chemical* **2019**, *278*, 126-132.
- [13] Murinzi, T. W.; Hosten, E.; Watkins, G. M., Synthesis and characterization of a cobalt-2,6-pyridinedicarboxylate MOF with potential application in electrochemical sensing. *Polyhedron* **2017**, *137*, 188-196.

- [14] Kang, X.; Wang, J.; Wu, H.; Aksay, I. A.; Liu, J.; Lin, Y., Glucose Oxidase–graphene–chitosan modified electrode for direct electrochemistry and glucose sensing. *Biosensors and Bioelectronics* **2009**, *25* (4), 901-905.
- [15] Misra, A., Carbon nanotubes and graphene-based chemical sensors. *Current Science* **2014**, *107* (3), 419-429.
- [16] Debataraja, A.; Muchtar, A. R.; Septiani, N. L. W.; Yulianto, B.; Nugraha; Sunendar, B., High Performance Carbon Monoxide Sensor Based on Nano Composite of SnO<sub>2</sub>-Graphene. *IEEE Sensors Journal* **2017**, *17* (24), 8297-8305.
- [17] Debataraja, A.; Septiani, N. L. W.; Yulianto, B.; Nugraha; Sunendar, B.; Abdullah, H., High performance of a carbon monoxide sensor based on a Pd-doped graphene-tin oxide nanostructure composite. *Ionics* **2019**, *25* (9), 4459-4468.
- [18] Luo, J.; Jiang, S.; Zhang, H.; Jiang, J.; Liu, X., A novel non-enzymatic glucose sensor based on Cu nanoparticle modified graphene sheets electrode. *Analytica Chimica Acta* **2012**, *709*, 47-53.
- [19] Lv, W.; Jin, F.-M.; Guo, Q.; Yang, Q.-H.; Kang, F., DNA-dispersed graphene/NiO hybrid materials for highly sensitive non-enzymatic glucose sensor. *Electrochimica Acta* **2012**, *73*, 129-135.
- [20] Alizadeh, T.; Mirzagholidpur, S., A Nafion-free non-enzymatic amperometric glucose sensor based on copper oxide nanoparticles–graphene nanocomposite. *Sensors and Actuators B: Chemical* **2014**, *198*, 438-447.
- [21] Mehek, R.; Iqbal, N.; Noor, T.; Nasir, H.; Mehmood, Y.; Ahmed, S., Novel Co-MOF/Graphene Oxide Electrocatalyst for Methanol Oxidation. *Electrochimica Acta* **2017**, *255*, 195-204.
- [22] Miles, D. O.; Jiang, D.; Burrows, A. D.; Halls, J. E.; Marken, F., Conformal transformation of [Co(bdc)(DMF)] (Co-MOF-71, bdc = 1,4-benzenedicarboxylate, DMF = N,N-dimethylformamide) into porous electrochemically active cobalt hydroxide. *Electrochemistry Communications* **2013**, *27*, 9-13.
- [23] Li, L.-X.; Xu, D.; Li, X.-Q.; Liu, W.-C.; Jia, Y., Excellent fluoride removal properties of porous hollow MgO microspheres. *New Journal of Chemistry* **2014**, *38* (11), 5445-5452.
- [24] Ansari, A.; Ali, A.; Asif, M.; Shamsuzzaman, Microwave-assisted MgO NP catalyzed one-pot multicomponent synthesis of polysubstituted steroidal pyridines. *New Journal of Chemistry* **2018**, *42* (1), 184-197.
- [25] Lou, X.; Chen, M.; Hu, B., The effect of nitrogen and oxygen coordination: toward a stable anode for reversible lithium storage. *New Journal of Chemistry* **2018**, *42* (19), 15698-15704.
- [26] Kurisingal, J. F.; Babu, R.; Kim, S.-H.; Li, Y. X.; Chang, J.-S.; Cho, S. J.; Park, D.-W., Microwave-induced synthesis of a bimetallic charge-transfer metal organic framework: a promising host for the chemical fixation of CO<sub>2</sub>. *Catalysis Science & Technology* **2018**, *8* (2), 591-600.
- [27] Shi, L.; Li, Y.; Cai, X.; Zhao, H.; Lan, M., ZIF-67 derived cobalt-based nanomaterials for electrocatalysis and non-enzymatic detection of glucose: Difference between the calcination atmosphere of nitrogen and air. *Journal of Electroanalytical Chemistry* **2017**, *799*, 512-518.
- [28] Yin, H.; Zhu, J.; Chen, J.; Gong, J.; Nie, Q., MOF-derived in situ growth of carbon nanotubes entangled Ni/NiO porous polyhedrons for high performance glucose sensor. *Materials Letters* **2018**, *221*, 267-270.
- [29] Zhang, X.; Xu, Y.; Ye, B., An efficient electrochemical glucose sensor based on porous nickel-based metal organic framework/carbon nanotubes composite (Ni-MOF/CNTs). *Journal of Alloys and Compounds* **2018**, *767*, 651-656.